A generalized stress intensity factor to be applied to rounded V-shaped notches

P. Lazzarin [a,*], S. Filippi [b]

[a] *Department of Management and Engineering, University of Padova, Stradella S.Nicola 3, 36100 Vicenza, Italy*
[b] *Department of Mechanical Engineering, University of Padova, Via Venezia 1, 35100 Padova, Italy*

Abstract

In the presence of sharp (zero radius) V-shaped notches the notch stress intensity factors (N-SIFs) quantify the intensities of the asymptotic linear elastic stress distributions. They are proportional to the limit of the mode I or II stress components multiplied by the distance powered $1 - \lambda_i$ from the notch tip, λ_i being Williams' eigenvalues. When the notch tip radius is different from zero, the definition is no longer valid from a theoretical point of view and the characteristic, singular, sharp-notch field diverges from the rounded-notch solution very next to the notch. Nevertheless, N-SIFs continue to be used as parameters governing fracture if the notch root radius is sufficiently small with respect to the notch depth.

Taking advantage of a recent analytical formulation able to describe stress distributions ahead of rounded V-notches, the paper gives a generalized form for the notch stress intensity factors, in which not only the opening angle but also the tip radius dimension is explicitly involved. Such parameters quantify the stress redistribution due to the root radius with respect to the sharp notch case.
© 2005 Elsevier Ltd. All rights reserved.

Keywords: Elasticity; Stress distributions; Generalized stress intensity factor; Crack; Corner; V-notch

1. Introduction

In the context of elasticity theory, the asymptotic stress state next to a re-entrant corner (sharp V-notch) is singular and the degree of singularity does depend on the notch opening angle (Williams, 1952). The stress field intensity is a function of the overall geometry of the component and the remotely applied loads,

---

* Corresponding author. Tel.: +39 0444 998780; fax: +39 0444 998888.
 E-mail address: plazzarin@gest.unipd.it (P. Lazzarin).

which is generally quantified by the notch stress intensity factors (hereafter N-SIFs). N-SIFs are the extension to sharp V-notches (Gross and Mendelson, 1972) of the conventional stress intensity factors used for cracks.

Any fracture criterion based on critical values of the notch stress intensity factor states that a crack propagates from the notch tip when the actual value of such parameter reaches a critical value. N-SIFs are endowed with an odd dimensionality, which depends on the notch angle (Williams, 1952) or on the elastic properties of bonded materials (Bogy, 1971). When the singularity degree is constant, the generalized stress intensity factors can be compared directly without any assumption regarding the actual entity that drives failure phenomenon. Reedy (1993) and Reedy and Guess (1993), for example, correlated failure of adhesive-bonded butt tensile joints with a generalized stress intensity at the free edge of the interface between elastic and rigid layers. The degree of singularity in those specimens was about −0.33, against −0.5 of linear elastic fracture mechanics.

The same degree of singularity, −0.33, was found to characterize a large amount of experimental data taken from the literature and related to steel and aluminum welded joints subjected to fatigue loading (Lazzarin and Tovo, 1998; Atzori et al., 1999; Lazzarin and Livieri, 2001). In those analyses the weld flank was modeled as a sharp V-notch with a constant value of the angle (135°), in order to overcome the variability of the weld toe radius and allow a strong synthesis of experimental data in terms of N-SIF, despite the large variability shown by main plate and transverse plate thickness, which ranged from 6 to 100 mm and from 3 to 200 mm, respectively.

By proceeding on parallel tracks, the problem of sharp V-notches in brittle or quasi-brittle materials under static loads, has been analyzed by many researchers (see, among the others, Carpinteri, 1987; Knesl, 1991; Seweryn, 1994; Nui et al., 1994; Chen, 1995, 1998; Fett, 1996; Dunn et al., 1997a,b; Lazzarin and Zambardi, 2001; Strandberg, 2002; Gómez and Elices, 2003a,b).

Knels and Seweryn's stress criterion of brittle failure is based on the assumption that crack initiation or propagation occurs when the mean value of decohesive stress over a specified damage segment d_0 reaches its critical value. (Knesl, 1991; Seweryn, 1994). Afterwards, the criterion was extended and applied also to structural elements under multi-axial loading (Seweryn and Mróz, 1995; Seweryn et al., 1997) by introducing a non local failure function capable of combining normal and shear stress components.

By using the body force method, Chen (1995) determined mode I and mode II N-SIFs for a variety of sharp V-notches and applied such factors to fracture analyses of plane specimens made of acrylic resin under mode I and mixed mode loading (Chen, 1998). Fracture at the notch tip was simulated by propagation of a small virtual crack, with a length of ε, positioned at the notch tip. Both the stress intensity factor at the virtual crack tip and the average energy release rate (for a crack with length of ε) were given as a function of mode I and mode II N-SIFs of uncracked specimens.

Re-analyzing a large amount of data reported in the literature, Gómez and Elices (2003a) observed that good agreement between computed and measured failure loads were obtained not only for ideally sharp notched (notch root radius equal to zero) and brittle fracture, but also when root radii were small (typically less than 0.05 mm) and when plasticity was contained. Afterwards, considering linear elastic behavior and ideally sharp notches, Gómez and Elices (2003b) were able to demonstrate that a single nondimensional curve provides an accurate fit of experimental data from V-notched specimens of steel, aluminum, PMMA and PVC. Their curve plots, as a function of the notch angle, the nondimensional parameter $K_{IC}^{*,V}$, which combines together critical value of N-SIFs, fracture toughness K_{IC} and a characteristic length of the material L_{ch}. Such a length depends on K_{IC} and the ultimate tensile stress σ_t according to the expression $L_{ch} = (K_{IC}/\sigma_t)^2$.

In general, the process zone must extend outside the region where the sharp and the blunt notch solutions deviate, so that failure can be considered governed by the singular terms of the elastic solution. Dealing with these problems, Dini and Hills (2004) have recently discussed in details the conditions under which the singular field characterizes the behavior of the finite radiused notch. The question Dini and Hills wished

specifically to address was the role played by notch intensity factors in characterizing the failure in the presence of a nearly sharp notch. They determined a lower and an upper bound to the load, both normalized to the shear yield stress, as a function of the notch angle, in order to achieve characterization of the process zone by the singular solution within a given discrepancy (5% or 10%). The lower bound to the load corresponded to a minimum value of the notch intensity factor and a maximum value of the root notch.

Recently Susmel and Taylor (2003) presented a number of experimental data obtained from tests conducted on V-notched specimens subjected to in-phase mixed mode I and mode II loadings. Since the mean value of the root radius was very small (0.074 mm) compared to the other notch dimensions, the notch stress intensity factors were conveniently determined by assuming a notch root radius equal to zero. However, by applying some critical distance methods, the best accuracy was obtained by Susmel and Taylor by taking into account the finite notch root radius, that is, by considering the real-elastic distribution ahead of the tested V-notches. That happened, in our opinion, because the root radius was not so different from the material length parameter $a_0 = 0.20$ mm.

As stated in the previous paragraph, definitions for N-SIFs given by Gross and Mendelson are valid only for ideally sharp V notches where Williams' solution exactly matches stress distributions; nevertheless these parameters are often adopted in the practice also in the presence of notch tip radii small but different from zero, by simply ignoring the presence of the radius. This assumption seems to be justified when the notch depth to tip radius ratio tends to infinite and, consequently, the blunt notch stress field slightly differs from the sharp notch stress distribution (the notch depth being kept constant). If the process zone governing fracture phenomena is greater than the zone influenced by the tip radius, N-SIF could be directly used to predict failure conditions.

The main aim of the present paper is to suggest a generalized form of N-SIFs capable of including the influence of the notch root radius and quantifying, in particular, the stress redistribution it involves. That will be obtained by leaving N-SIF's unit unchanged in that this will continue to be governed by Williams' solution as for the sharp notch case. The new factors will be obtained taking advantage of a complex potential solution recently reported in the literature (Filippi et al., 2002). Since that formulation was not exact but approximate, the accuracy of the new definitions will be carefully checked against numerical analyses.

Finally, some plots correlating mode I N-SIFs for radiused notches to the conventional N-SIFs for sharp notches will be presented as a function of ρ/a and h/a ratios, ρ and a being the notch root radius and depth, and h the ligament width.

2. Analytical background

By using stress distributions along the notch bisector ($\theta = 0$), Modes I and II generalized stress intensity factors for sharp V notches are given by the following expressions (Gross and Mendelson, 1972):

$$K_{\mathrm{I}}^{\mathrm{V}} = \sqrt{2\pi} \lim_{r \to 0} r^{1-\lambda_1} [\sigma_\theta(r,0)] \tag{1}$$

$$K_{\mathrm{II}}^{\mathrm{V}} = \sqrt{2\pi} \lim_{r \to 0} r^{1-\lambda_2} [\tau_{r\theta}(r,0)] \tag{2}$$

where λ_1 and λ_2 are Williams' eigenvalues. In another, slightly different, definition reported in the literature the exponents $(1 - \lambda_i)$ embrace also (2π) (Carpinteri, 1987; Seweryn, 1994).

Eqs. (1) and (2) involve stress distributions present on the notch bisector, where symmetric and skew-symmetric stress distributions can be separated, and formulated as limit condition in order to avoid any influence of the remote stress field. There is, however, a finite size region where stresses and strains are fully controlled by N-SIFs.

Thanks to Williams' solution, definitions (1) and (2) are exact for sharp V-notch problems. On the other hand, their extension to non-zero-radius V-notches is somewhat arbitrary. Due to the presence of the rounded notch root, when the distance r from the notch tip tends to zero, also Eqs. (1) and (2) tends to zero. To overcome this problem, N-SIFs (1) and (2) are commonly evaluated at a convenient distance from the notch tip, where the tip radius influence strongly decreases and the slopes of stress fields match quite well those of sharp V-notches. This behavior is shown in Fig. 2a where, at distances from the notch tip greater than about 0.5ρ, FE stress distributions for the blunt notches exhibit a constant slope in a double logarithmic diagram. In this zone the intensity of the stress field can be expressed in term of NSIF. On the other hand, the degree of accuracy and the limits of this approach are not clearly identified. The limits are evident in Fig. 2b, where the product $\sqrt{2\pi}r^{1-\lambda_1}[\sigma_\theta(r,0)]$, see Eq. (1), is plotted for different U-notches in a finite size plate. It is evident that the extension of the region where N-SIF is almost constant or where it does not vary significantly depends on the notch geometry: the greater the tip radius value, the lower the zone size. This zone completely disappears when the tip radius has the same order of magnitude of the notch depth (2.5 mm against 10.0 mm, see Fig. 2b). Only when $\rho = 0$ Eq. (1) an exact value for Mode I NSIF.

The problem is even more complicated in the presence of mode II load conditions. In the presence of a notch tip radius different from zero, equilibrium conditions at the notch root force $\tau_{r\theta}$ to be null at the edge, while the stress distribution due to sharp notch remains singular, at least when the notch angle is less than 102° (Williams, 1952).

Filippi et al. (2002) recently proposed an analytical approach for describing local stress field ahead of rounded V-notches. The stress components were written by separating the contribution caused by the symmetric solution (mode I) from that caused by to the skew-symmetric solution (mode II).

With reference to the coordinate system shown in Fig. 1, mode I stresses are (Filippi et al., 2002):

$$
\begin{Bmatrix} \sigma_\theta \\ \sigma_r \\ \tau_{r\theta} \end{Bmatrix} = \lambda_1 r^{\lambda_1 - 1} a_1 \left[\left\{ \begin{Bmatrix} (1+\lambda_1)\cos(1-\lambda_1)\theta \\ (3-\lambda_1)\cos(1-\lambda_1)\theta \\ (1-\lambda_1)\sin(1-\lambda_1)\theta \end{Bmatrix} + \chi_{b_1}(1-\lambda_1) \begin{Bmatrix} \cos(1+\lambda_1)\theta \\ -\cos(1+\lambda_1)\theta \\ \sin(1+\lambda_1)\theta \end{Bmatrix} \right\} \right.
$$
$$
\left. + \frac{q}{4(q-1)}\left(\frac{r}{r_0}\right)^{\mu_1-\lambda_1} \left(\chi_{d_1} \begin{Bmatrix} (1+\mu_1)\cos(1-\mu_1)\theta \\ (3-\mu_1)\cos(1-\mu_1)\theta \\ (1-\mu_1)\sin(1-\mu_1)\theta \end{Bmatrix} + \chi_{c_1} \begin{Bmatrix} \cos(1+\mu_1)\theta \\ -\cos(1+\mu_1)\theta \\ \sin(1+\mu_1)\theta \end{Bmatrix} \right) \right]
\tag{3}
$$

where both the real number q and the distance r_0 from the origin of the coordinate system and notch tip depend on the V-notch angle according to the expressions reported in Fig. 1. These expressions were derived by Lazzarin and Tovo (1996) and Filippi et al. (2002) by using Neuber's conformal mapping in an auxiliary (u,v) semi-infinite plane (Neuber, 1958). It might be sufficient to remember here that the relation
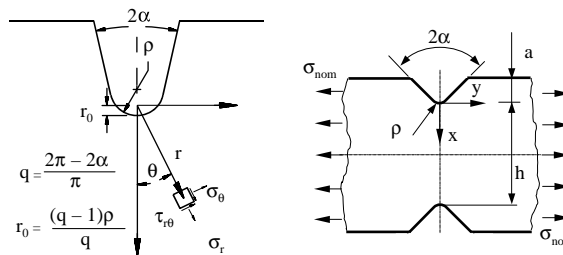

Fig. 1. Coordinate systems and geometrical parameters. Distance r_0 defined according to Lazzarin and Tovo (1996) and Filippi et al. (2002).
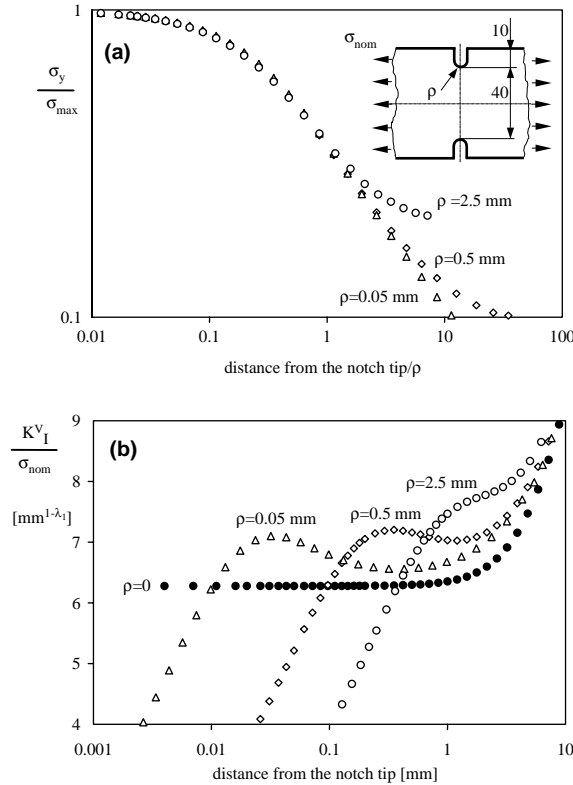
Fig. 2. Plots of the maximum principal stress (a) and Mode I notch intensity factor along the notch bisector (b). K_1^V expressed according to Eq. (1) while eliminating the limit condition $r \to 0$.

between Cartesian coordinates and curvilinear coordinates is $x + \mathrm{i}y = (u + \mathrm{i}v)^q$, where q is a real number ranging from 1.0 (flat edge) to 2.0 (crack). Then the curve defined by $u = 0$, which describes an angle equal to 2α, allows us to determine the relationship between q and 2α. On the other hand, by using the curve $u = u_0$ approximating the free edge of the notch and, in particular, the relationship $r_0 = (u_0)^q$, it is possible to obtain the link between radius of curvature ρ and distance r_0. Since Eq. (3) represents the symmetric solution, the $\tau_{r\theta}$ stress component is always null along the notch bisector.

Mode II stresses are

$$
\begin{Bmatrix} \sigma_\theta \\ \sigma_r \\ \tau_{r\theta} \end{Bmatrix} = \lambda_2 r^{\lambda_2 - 1} a_2 \left[\left\{ \begin{matrix} (1+\lambda_2)\sin(1-\lambda_2)\theta \\ (3-\lambda_2)\sin(1-\lambda_2)\theta \\ (1-\lambda_2)\cos(1-\lambda_2)\theta \end{matrix} \right\} + \chi_{b_2}(1+\lambda_2)\left\{ \begin{matrix} \sin(1+\lambda_2)\theta \\ -\sin(1+\lambda_2)\theta \\ \cos(1+\lambda_2)\theta \end{matrix} \right\} \right.
$$
$$
\left. + \frac{1}{4(\mu_2-1)}\left(\frac{r}{r_0}\right)^{\mu_2-\lambda_2}\left(\chi_{d_2}\left\{ \begin{matrix} (1+\mu_2)\sin(1-\mu_2)\theta \\ (3-\mu_2)\sin(1-\mu_2)\theta \\ (1-\mu_2)\cos(1-\mu_2)\theta \end{matrix} \right\} + \chi_{c_2}\left\{ \begin{matrix} -\sin(1+\mu_2)\theta \\ \sin(1+\mu_2)\theta \\ -\cos(1+\mu_2)\theta \end{matrix} \right\} \right) \right] \qquad (4)
$$

Now, along the notch bisector, stress components σ_θ and σ_r are null.

In Eqs. (3) and (4) the constants a_1 and a_2 need to be evaluated on the basis of the local stress distributions. All the other parameters in Eqs. (3) and (4) have closed form expressions (Filippi et al., 2002) but here, for brevity's sake, such expressions are omitted and only the values assumed by the parameters for some typical notch angles are reported in Table 1.

Table 1
Parameters for mode I and mode II stress components

2α (degrees)	q	λ_1 λ_2	μ_1 μ_2	χ_{b_1} χ_{b_2}	χ_{c_1} χ_{c_2}	χ_{d_1} χ_{d_2}	$\tilde{\omega}_1$ $\tilde{\omega}_2$
0	2	0.5	−0.5	1	4	0	1
		0.5	−0.5	1	−12	0	−1
30	1.833	0.501	−0.456	1.071	3.791	0.063	1.034
		0.598	−0.447	0.921	−11.350	−0.351	−1
45	1.750	0.505	−0.432	1.166	3.572	0.083	1.014
		0.660	−0.412	0.814	−10.188	−0.451	−1
60	1.667	0.512	−0.406	1.312	3.283	0.096	0.970
		0.731	−0.373	0.658	−8.395	−0.479	−1
90	1.5	0.545	−0.345	1.841	2.506	0.105	0.810
		0.909	−0.288	0.219	−2.938	−0.244	−1
120	1.333	0.616	−0.268	3.003	1.515	0.087	0.570
		1.149	−0.198	−0.314	4.560	0.513	−1
135	1.25	0.674	−0.220	4.153	0.993	0.067	0.432
		1.302	−0.151	−0.570	8.737	1.136	−1

Consider now only stress components σ_θ and $\tau_{r\theta}$ along the notch bisector ($\theta = 0$). They are given by

$$(\sigma_\theta)_{\theta=0} = \sigma_y = \lambda_1 r^{\lambda_1-1} a_1 [1 + \lambda_1 + \chi_{b_1}(1 - \lambda_1)] \left\{ 1 + \tilde{\omega}_1 \left(\frac{r}{r_0}\right)^{\mu_1-\lambda_1} \right\} \tag{5}$$

$$(\tau_{r\theta})_{\theta=0} = \tau_{xy} = \lambda_2 r^{\lambda_2-1} a_2 [1 - \lambda_2 + \chi_{b_2}(1 + \lambda_2)] \left\{ 1 + \tilde{\omega}_2 \left(\frac{r}{r_0}\right)^{\mu_2-\lambda_2} \right\} \tag{6}$$

where

$$\tilde{\omega}_1 = \frac{q}{4(q-1)} \left[\frac{\chi_{d_1}(1 + \mu_1) + \chi_{c_1}}{1 + \lambda_1 + \chi_{b_1}(1 - \lambda_1)} \right] \tag{7}$$

$$\tilde{\omega}_2 = \frac{1}{4(\mu_2-1)} \left[\frac{\chi_{d_2}(1 - \mu_2) - \chi_{c_2}}{1 - \lambda_2 + \chi_{b_2}(1 + \lambda_2)} \right] = -1.0 \tag{8}$$

Parameter $\tilde{\omega}_1$ is tabulated in the last column of Table 1 where, as for Eqs. (3)–(6), indexes 1, 2 are associated to mode I and mode II stress distributions, respectively. Table 1 shows that $\tilde{\omega}_1$ is almost constant when 2α is equal to or less than 60°; beyond this angle $\tilde{\omega}_1$ progressively decreases as 2α increases. This means that in the presence of large V-notch angles the blunt V-notch solution tends to the sharp V-notch solution more rapidly than as to low angle cases. In order to better clarify the effect of the terms related to the eigenvalue μ, (such terms vanishes when $\rho = 0$) it is necessary to consider not only the variability of $\tilde{\omega}_1$ but also that of the distance r_0. Let us define the parameters:

$$C_{\mu 1} = \left(\frac{r_0 + x}{x}\right)^{\lambda_1} \left[1 + \tilde{\omega}_1 \left(\frac{r_0 + x}{r_0}\right)^{\mu_1-\lambda_1} \right] \tag{9}$$

$$C_{\mu 2} = \left(\frac{r_0 + x}{x}\right)^{\lambda_2} \left[1 + \tilde{\omega}_2 \left(\frac{r_0 + x}{r_0}\right)^{\mu_2-\lambda_2} \right] \tag{10}$$

Table 2
Minimum value of the distance $\bar{x}$ from the notch tip at which is 2% or 5% the difference between Eq. (3) and Williams' solution based only on the $r^{1-\lambda}$ term

	$2\alpha = 0°$	$2\alpha = 30°$	$2\alpha = 45°$	$2\alpha = 60°$	$2\alpha = 90°$	$2\alpha = 120°$	$2\alpha = 135°$
$C_{\mu 1} = 5\%$	3.73ρ	4.89ρ	5.04ρ	4.84ρ	3.27ρ	$<\rho$	$<\rho$
$C_{\mu 1} = 2\%$	11.33ρ	15.01ρ	15.87ρ	15.74ρ	11.87ρ	4.79ρ	1.71ρ
$C_{\mu 2} = 5\%$	14.37ρ	10.99ρ	9.29ρ	7.57ρ	4.25ρ	1.53ρ	0.63ρ
$C_{\mu 2} = 2\%$	36.87ρ	27.51ρ	22.91ρ	18.35ρ	9.72ρ	3.00ρ	1.03ρ

where x is the distance from the notch tip (Fig. 1). Such parameters allow us to quantify the errors committed in the evaluation of N-SIFs when the presence of the notch tip radius is neglected and only the terms proportional to $r^{1-\lambda}$ of Eq. (1) are used. Table 2 displays the minimum distance $\bar{x}$ able to assure a 2% or 5% maximum mismatch. The finiteness of the plates is not considered in this evaluation. It is evident that, by increasing the notch angle, $\bar{x}$ decreases and the effect is particularly evident when the angle is greater than 90°.

3. An alternative formulation

With reference only to mode I stress distributions, a first, partial solution to the above said problems, can be obtained by linking the generalized stress intensity factor to the maximum principal stress at the notch tip, $\sigma_{\max}$, by means of the following expression (Filippi et al., 2002):

$$K^{V}_{\rho,I} = \sigma_{\max}\sqrt{2\pi}\frac{r_0^{1-\lambda_1}}{1+\tilde{\omega}_1} = \sigma_{\max}\frac{\sqrt{2\pi}}{1+\tilde{\omega}_1}\left(\frac{q-1}{q}\rho\right)^{1-\lambda_1} \tag{11}$$

When the notch angle is null, $q = 2$, $\tilde{\omega}_1$, $r_0 = \rho/2$, so that Eq. (11) immediately gives $K^{V}_{\rho,I} = \sigma_{\max}\sqrt{\pi\rho}/2$ (Irwin, 1958; Glinka, 1985). Under mode II conditions, the procedure cannot be applied, because $\tau_{r\theta}$ at the notch tip is always zero.

In the presence of mode I loading, the generalized stress intensity factor $K^{V}_{\rho,I}$ should be compared with a given critical value, characteristic of each material, notch angle, notch radius and, in more general terms, temperature and strain rate (Gómez and Elices, 2004).

Recently, Eq. (11) has been extensively used by Gómez and Elices (2004) who were able to summarize a large amount of data obtained from three-point and four point bending, as well as single and double edge notched bars subject to traction. Materials were PMMA, steel and some ceramics. The relation between $K^{V}_{\rho,I}$ and its critical value, denoted therein as $K^{\rho V}_C$, was determined by using the cohesive zone model, from the knowledge of the elastic properties of the materials (Young's modulus and Poisson's coefficient) and their softening functions.

In order to formulate a more general approach, useful also for blunt notches under mixed load conditions, we suggest that the stresses ahead of the notch tip should be used instead of the peak stress on it, Eq. (11). Definitions for mode I and mode II generalized N-SIFs are then

$$K^{V}_{\rho,I} = \sqrt{2\pi}r^{1-\lambda_1}\frac{(\sigma_\theta)_{\theta=0}}{1+\tilde{\omega}_1\left(\frac{r}{r_0}\right)^{\mu_1-\lambda_1}} \tag{12}$$

$$K^{V}_{\rho,II} = \sqrt{2\pi}r^{1-\lambda_2}\frac{(\tau_{r\theta})_{\theta=0}}{1+\tilde{\omega}_2\left(\frac{r}{r_0}\right)^{\mu_2-\lambda_2}} \tag{13}$$

where σ_θ and $\tau_{r\theta}$ are the stresses at the distance r from the local frame origin (Fig. 1).

Eqs. (12) and (13) might be seen as the extension to rounded V-notches of Gross and Mendelson's definition for sharp V-notches. It is worth noting that Williams's solution for sharp V-notches is exact, while Eqs. (3) and (4) are approximate because they satisfy boundary conditions not on the entire free edge but at the notch tip and at convenient distance from it (Filippi et al., 2002). Consequently, Eqs. (12) and (13) are not expected to give a constant value for N-SIFs. They will rather show a slightly oscillating value ahead of the notch tip. The entity of this oscillation is shown in Fig. 3 for two U-notched plates. $K_{\rho,I}^V$ is normalized with respect to the nominal stress and plotted against the distance from the notch tip. The figure shows that the size of the region where $K_{\rho,I}^V$ exhibits a weak variability is approximately 1 mm, i.e. 1/10 of the notch depth. The ratio $K_{\rho,I}^V/\sigma_{nom}$ ranges from 6.94 to 7.00 when $\rho = 2.5$ mm, from 6.43 to 6.62 when $\rho = 0.5$ mm. The maximum differences are 1% and 3%, respectively.

Fig. 4 shows the same comparison in plates with V-notches characterized by $2\alpha = 135°$. Up to a distance from the notch tip equal to 1.0 mm, the ratio $K_{\rho,I}^V/\sigma_{nom}$ ranges from 6.16 to 6.43 ($\rho = 0.5$ mm) and from 6.27 to 6.46 ($\rho = 2.5$ mm). Differences are then 4.5% and 3%, respectively.

In order to eliminate the weak dependence on the notch tip distance, the mean values, defined as follows:

$$\overline{K}_{\rho,I}^V = \frac{1}{\eta\rho} \int_{r_0}^{r_0+\eta\rho} (K_{\rho,I}^V)\, \mathrm{d}r \tag{14}$$

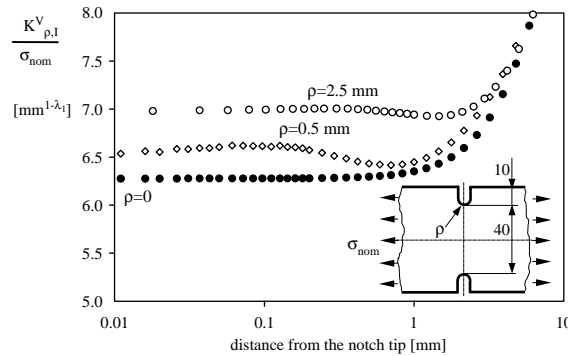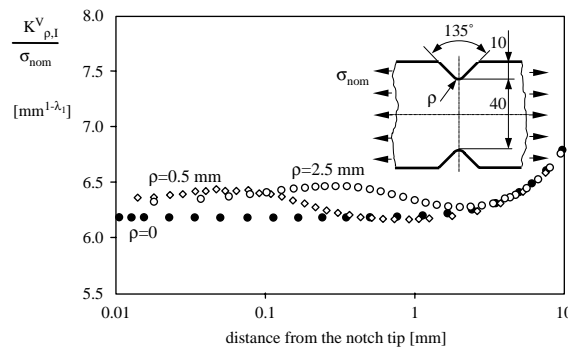Fig. 3. Plots of $K_{\rho,I}^V$, Eq. (12), for some U-notched plates.

Fig. 4. Plots of $K_{\rho,I}^V$, Eq. (12), for some V-notched plates with $2\alpha = 135°$.

$$\overline{K}_{\rho,\mathrm{II}}^{\mathrm{V}} = \frac{1}{\eta\rho} \int_{r_0}^{r_0+\eta\rho} (K_{\rho,\mathrm{II}}^{\mathrm{V}}) \, \mathrm{d}r \tag{15}$$

might be used.

In the analyses reported below, η will be set equal to 0.4, i.e. the upper bound value suitable to avoid any influence of the nominal stress region in problems where the stress concentration effects are low (Atzori et al., 2001). A number of FE analyses will permit a direct comparison between Eqs. (12) and (14), justifying the adoption of the engineering parameter $K_{\rho,\mathrm{I}}^{\mathrm{V}}$ for rapid estimations of stress distribution intensity.

As soon as N-SIFs are determined, parameters a_1, a_2 in Eqs. (3)–(6) can be immediately derived according to the following expressions:

$$a_1 = \frac{K_{\rho,\mathrm{I}}^{\mathrm{V}}}{\lambda_1 \sqrt{2\pi}[1 + \lambda_1 + \chi_{b_1}(1 - \lambda_1)]} \tag{16}$$

$$a_2 = \frac{K_{\rho,\mathrm{II}}^{\mathrm{V}}}{-\lambda_2 \sqrt{2\pi}[1 - \lambda_2 + \chi_{b_1}(1 + \lambda_2)]} \tag{17}$$

4. Comparison with finite element results

In order to investigate the suitability of previous definitions, a number of different models were investigated numerically. A first set of analyses addressed mode I problems. With reference to geometrical parameters shown in Fig. 1 and Table 3 summarizes the geometrical features of a number of models weakened by V-notches together with their theoretical stress concentration factors (maximum principal stress at the notch tip to nominal stress ratio), referred either to the gross area or the net area of the models. According to suggestions reported by Filippi and Lazzarin (2004), in order to minimize the errors, also U notches were treated as a V-notches with a fictitious opening angle $2\alpha_{\mathrm{eq}} = 30°$.

In the last column of the Table 3 is reported the distance $\bar{\bar{x}}$ beyond which the finite size effect (FSE) causes a mismatch with the theoretical solution. To do so, we assigned $C_{\mathrm{FSE}} = 0.05$, the parameter being defined according to the following expression:

$$C_{\mathrm{FSE}} = \frac{\sigma_{\mathrm{y\ FEM}} - \sigma_{\mathrm{y\ Eq.\ (5)}}}{\sigma_{\mathrm{y\ Eq.\ (5)}}} \tag{18}$$

The results in Table 3 show that:

- by keeping ρ, a and 2α constant, $\bar{\bar{x}}$ increases with the ligament width h;
- by keeping a, h and 2α constant, $\bar{\bar{x}}$ increases with ρ;
- by keeping ρ, a and h constant, $\bar{\bar{x}}$ increases with 2α.

Table 4 gives values of $K_{\rho,\mathrm{I}}^{\mathrm{V}}$ provided by Eq. (12) at very different distances from the notch tip. The last column also displays the parameter's mean value evaluated by means of Eq. (14). It is worth noting that in all cases considered here the engineering parameter is close to its mean value. The difference between local values and mean values never exceeds $\pm3.5\%$. This means that $K_{\rho,\mathrm{I}}^{\mathrm{V}}$ is surely a tool of interest, suitable for applications. It should be also noted that at a distance from the notch tip equal to 0.2ρ or 0.3ρ the difference between $K_{\rho,\mathrm{I}}^{\mathrm{V}}$ and $\overline{K}_{\rho,\mathrm{I}}^{\mathrm{V}}$ is always less than 1%.

Figs. 5 and 6 show the results of a second set of analyses carried out on geometries where the notch subjected to mixed mode load conditions. Also in these cases there exists a finite size zone where stress field

Table 3
Geometrical parameters and stress concentration factors referred to the gross area (K_{tgross}) and the net area (K_{tnet}), being valid the expression $K_{tgross} = K_{tnet} (h + 2a)/h$

Model no.	Type of notch (2α)	Notch depth a	Notch tip radius ρ	Ligament width h	K_{tgross}	K_{tnet}	Distance $\bar{\bar{x}}$
1	U	5	2.5	20	3.96	2.64	0.29a
2	U	10	2.5	20	5.58	2.79	0.33a
3	U	10	2.5	40	5.33	3.56	0.43a
4	U	10	1.25	40	7.26	4.84	0.35a
5	U	10	0.5	40	11.12	7.41	0.27a
6	U	10	0.5	80	11.32	9.05	0.30a
7	V (45°)	5	2.5	20	3.96	2.64	0.26a
8	V (45°)	10	2.5	40	5.33	3.55	0.36a
9	V (45°)	10	1.25	40	7.25	4.83	0.29a
10	V (45°)	10	0.5	40	11.09	7.40	0.22a
11	V (90°)	5	2.5	20	3.94	2.63	0.25a
12	V (90°)	10	2.5	40	5.27	3.51	0.37a
13	V (90°)	10	1.25	40	7.08	4.72	0.33a
14	V (90°)	10	0.5	40	10.61	7.07	0.28a
15	V (135°)	5	2.5	20	3.57	2.38	0.56a
16	V (135°)	10	2.5	20	4.83	2.42	0.39a
17	V (135°)	10	2.5	40	4.50	3.00	0.78a
18	V (135°)	10	2.5	80	4.58	3.66	1.27a
19	V (135°)	10	0.5	20	8.10	4.05	0.38a
20	V (135°)	10	0.5	40	7.57	5.04	0.74a
21	V (135°)	10	0.5	80	7.70	6.16	1.19a

All models present a double symmetry. Distance $\bar{\bar{x}}$ evaluated for $C_{FSE} = 0.05$.

Table 4
Values of $K_{\rho,I}^V$ for a nominal stress $\sigma_{nom} = 1$ MPa

Model no.	($K_{\rho,I}^V$ according to Eq. (12)) $[mm]^{1-\lambda_1}$ $(r-r_0)/\rho$									$\overline{K}_{\rho,I}^V$ $[mm]^{1-\lambda_1}$ Eq. (14)
	0	0.1	0.2	0.3	0.4	0.5	0.7	1.0	3.0	
1	2.33	2.33	2.31	2.31	2.30	2.31	2.34			2.32
2	7.39	7.39	7.39	7.39	7.38	7.39	7.43	7.57		7.38
3	7.01	7.04	7.02	6.99	6.97	6.95	6.96	7.04		7.01
4	6.75	6.81	6.80	6.77	6.74	6.72	6.68	6.67		6.81
5	6.55	6.63	6.64	6.63	6.60	6.56	6.51	6.45	6.58	6.62
6	6.66	6.75	6.78	6.75	6.71	6.68	6.61	6.55	6.66	6.74
7	2.30	2.31	2.30	2.30	2.30	2.31	2.34			2.30
8	6.87	6.94	6.95	6.94	6.92	6.91	6.96			6.93
9	6.63	6.74	6.74	6.73	6.69	6.66	6.65			6.72
10	6.44	6.56	6.59	6.59	6.66	6.54	6.49	6.44	6.57	6.56
11	2.41	2.47	2.48	2.48	2.47	2.47	2.49			2.47
12	6.72	6.90	6.95	6.94	6.92	6.90	6.89	6.91		6.90
13	6.58	6.78	6.83	6.83	6.80	6.77	6.72	6.67		6.78
14	6.49	6.70	6.76	6.75	6.72	6.68	6.62	6.56	6.61	6.70
15	2.95	3.03	3.01	2.98	2.96	2.95	2.94	2.95		3.00
16	6.29	6.46	6.43	6.38	6.34	6.31	6.28	6.28		6.41
17	6.39	6.57	6.53	6.47	6.42	6.38	6.34	6.30	6.45	6.51
18	6.75	6.95	6.94	6.90	6.87	6.86	6.87	6.93		6.91
19	6.25	6.42	6.39	6.33	6.28	6.25	6.21	6.18	6.19	6.37
20	6.36	6.53	6.50	6.44	6.39	6.35	6.31	6.27	6.25	6.47
21	6.68	6.87	6.84	6.79	6.73	6.70	6.65	6.64	6.73	6.82

Fig. 5. $K_{\rho,\mathrm{I}}^{\mathrm{V}}$ and $K_{\rho,\mathrm{II}}^{\mathrm{V}}$, Eqs. (12) and (13), plotted along the notch bisector.

Fig. 6. $K_{\rho,\mathrm{I}}^{\mathrm{V}}$ and $K_{\rho,\mathrm{II}}^{\mathrm{V}}$, Eqs. (12) and (13), plotted along the notch bisector of a weld-like geometry.

parameters $K_{\rho,\mathrm{I}}^{\mathrm{V}}$ and $K_{\rho,\mathrm{II}}^{\mathrm{V}}$ show a weak variability. The region size for $K_{\rho,\mathrm{I}}^{\mathrm{V}}$ is about 1.0 mm, this value is to be compared with the height of the notch flanks (10 mm). In such a region $K_{\rho,\mathrm{I}}^{\mathrm{V}}$ ranges from 2.68 to 2.77 in Fig. 5 and from 3.58 to 3.68 in Fig. 6. For $K_{\rho,\mathrm{II}}^{\mathrm{V}}$ the region size is far more variable; it strongly increases when the distribution of the corresponding sharp V-notch case is no longer singular.

5. Some expressions linking sharp notches to rounded notches

A collection of stress intensity factors for cracks in finite and infinite plates, at stress concentration zones of notches and welded joints, as well as at the interface and the corners of dissimilar materials is given by Murakami (2001).

By extending the celebrated Creager and Paris' formulation from blunt cracks (Creager and Paris, 1967) to common notches, Glinka correlated mode I generalized stress intensity factor and maximum elastic stress at the notch tip by the expression (Glinka, 1985)

$$\sigma_{\max} = 2\frac{K_I}{\sqrt{\pi\rho}} \tag{19}$$

Eq. (19) can be satisfactory applied also to narrow V-notches, due to the weak variability of degree of singularity when $2\alpha < 90°$.

For large V notches a more general expression can be derived from Eq. (11). This expression represents a generalized form of Eq. (19) and can be applied also when the root radius is comparable to notch depth:

$$\sigma_{\max} = (1 + \tilde{\omega}_1)\frac{K_{\rho,\mathrm{I}}^{\mathrm{V}}}{\sqrt{2\pi}r_0^{1-\lambda_1}} \tag{20}$$

Generally, in the presence of a very small value of notch tip radius, $K_{\rho,\mathrm{I}}^{\mathrm{V}}$ is substituted by $K_{\mathrm{I}}^{\mathrm{V}}$. However, we typically have $K_{\rho,\mathrm{I}}^{\mathrm{V}} \geqslant K_{\mathrm{I}}^{\mathrm{V}}$, thus the introduction of $K_{\mathrm{I}}^{\mathrm{V}}$ into Eq. (20) might result in an underestimation of the elastic peak stress.

A number of numerical analyses have been carried out to correlate the N-SIFs related to sharp and rounded V-notches. All analyses have considered symmetric plates with double edge notches characterized by

- ρ/a equal to 0.0, 0.02, 0.04, 0.08, 0.16, 0.32 and 0.64;
- h/a equal to 2, 5, 10 and 50;
- notch angle equal to 30°, 45°, 60°, 90°, 120° and 135°.

In all cases (168 models), N-SIFs for rounded notches were calculated by means of Eq. (12). In order to make calculations more rapid, we used a distance from the notch tip equal to 0.2ρ. The results already reported in Table 4 justified that choice. The new results are shown in Fig. 7a–f where symbols refer to different h/a ratios. It is worth noting that the $K_{\rho,\mathrm{I}}^{\mathrm{V}}/K_{\mathrm{I}}^{\mathrm{V}}$ ratio exhibits a weak dependence on the ligament width when $h/a \geqslant 5$. For these cases, the ratio between the N-SIFs can be simply given as a function of ρ/a.

As a consequence, contributions to local stress distribution due to global and local geometry can be separated. More precisely, global parameters, such as the remote applied load, the notch opening angle and the h/a ratio, directly influence the N-SIF value of the equivalent sharp notch, but they do not give a substantial contribution to the $K_{\rho,\mathrm{I}}^{\mathrm{V}}/K_{\mathrm{I}}^{\mathrm{V}}$ ratio, which can be evaluated only on the basis of the local geometry (ρ/a ratio). These outcomes are rigorously valid only for pure mode I loading but they can be extended also to mixed mode loading, at least when the mode II stress contribution is low or when the corresponding sharp V-notch case exhibits non-singular stress distributions.

In order to provide a tool suitable to estimate the $K_{\rho,\mathrm{I}}^{\mathrm{V}}/K_{\mathrm{I}}^{\mathrm{V}}$ ratio as a function of ρ/a, we suggest here the simple linear law:

$$K_{\rho,\mathrm{I}}^{\mathrm{V}}/K_{\mathrm{I}}^{\mathrm{V}} = \varphi + \psi\frac{\rho}{a} \tag{21}$$

where both φ and ψ depend on the opening angle (Table 5).

Fig. 7a–f plots Eq. (21), obtained by interpolating the FE data related to the case with $h/a = 50$ (which better approximates the limit case of a finite size notch in semi-infinite plate). However, the curve represents a good approximation for all cases with h/a equal to or greater than 5.0.

By fitting the data reported in Table 5 a rapid estimation of φ and ψ can be achieved by the following expressions:

$$\varphi(\alpha) = 1.372(1.00115)^{\alpha}\alpha^{-0.0906} \quad \psi(\alpha) = 0.0972 + 0.163\cos(0.01525\alpha) \tag{22}$$

where α is in degrees. Plots of φ and ψ are shown in Fig. 8.

As an example of application of Eqs. (21) and (22), six plots of σ_{θ} stress component on the notch bisector are shown in Fig. 9. Notch root radius ρ is 0.4 mm (Fig. 9a) and 3.2 mm (Fig. 9b), while the notch depth and ligament width are kept constant. For the relevant sharp notch cases, FE analyses gave $K_{\mathrm{I}}^{\mathrm{V}} = 6.41 \text{ MPa(mm)}^{0.495}$ for $2\alpha = 45°$, $K_{\mathrm{I}}^{\mathrm{V}} = 6.49 \text{ MPa(mm)}^{0.384}$ for $2\alpha = 120°$ and $K_{\mathrm{I}}^{\mathrm{V}} = 6.16 \text{ MPa(mm)}^{0.326}$ for
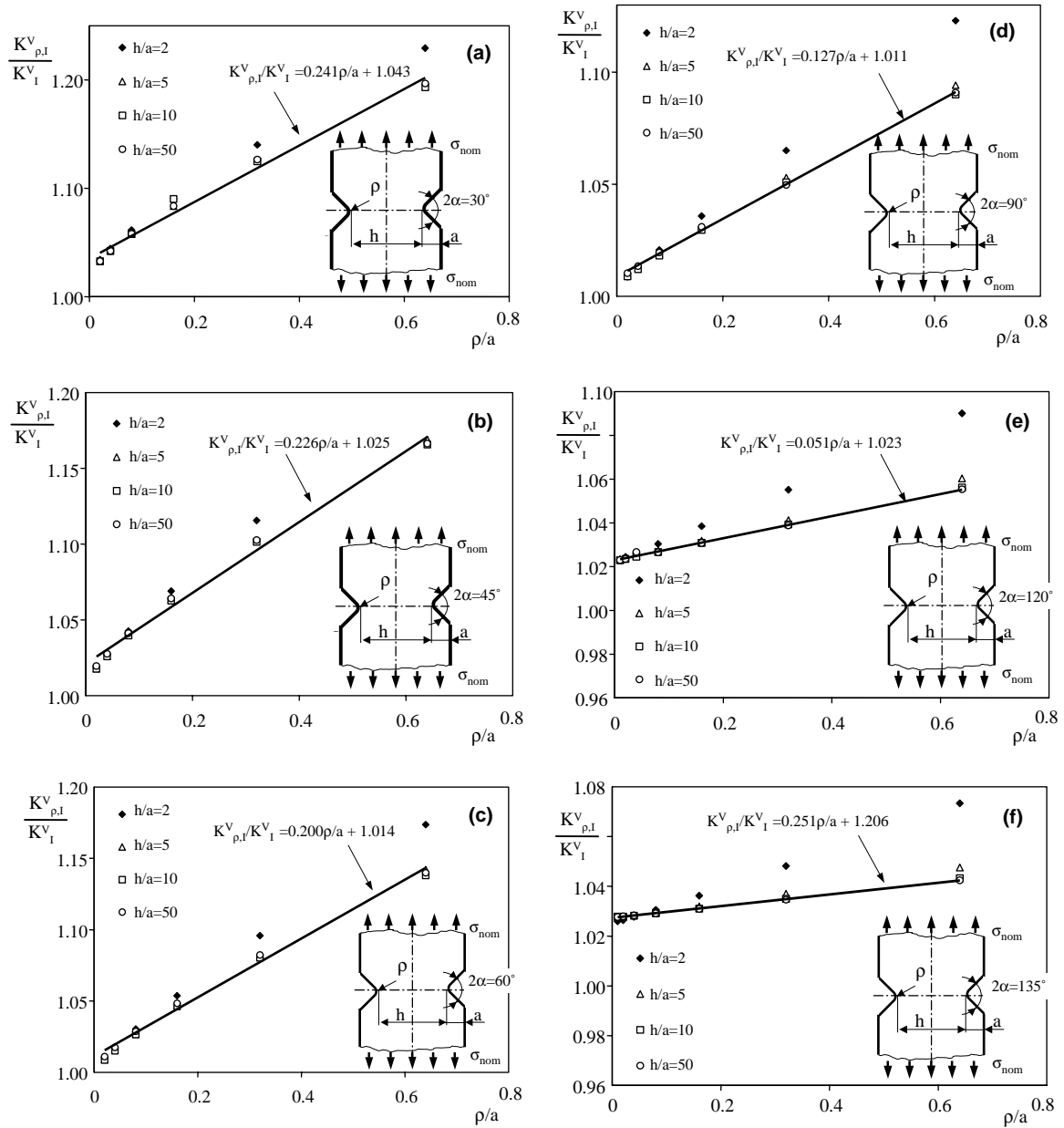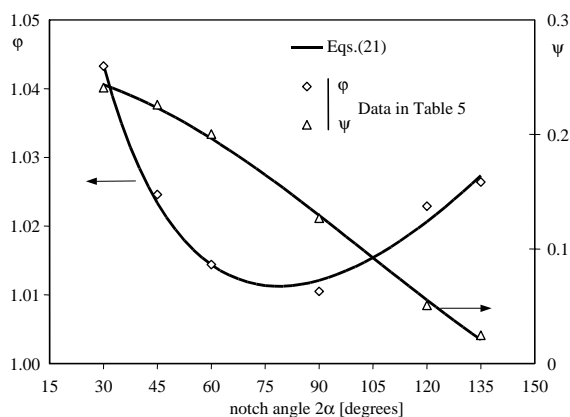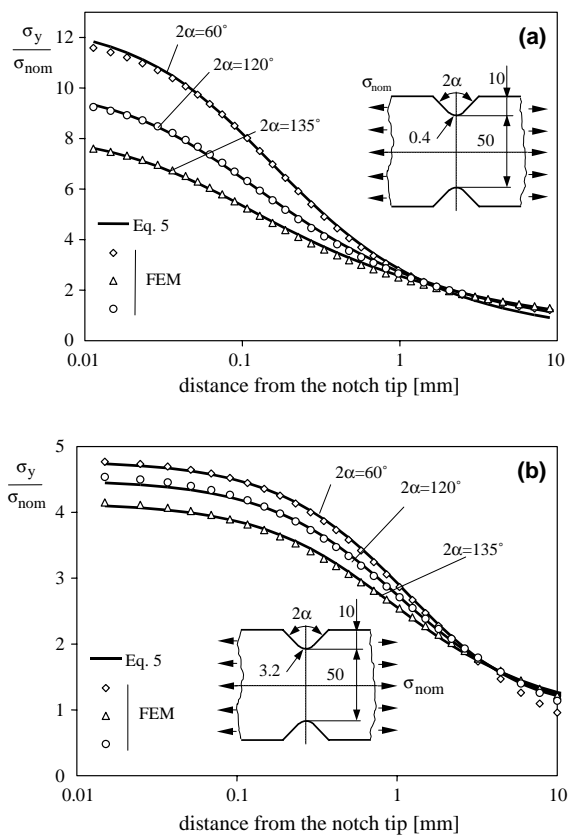
Fig. 7. $K_{\rho,I}^V/K_I^V$ for plates weakened by double V-notches. Notch angle: $2\alpha = 30°$ (a), $2\alpha = 45°$ (b), $2\alpha = 60°$ (c), $2\alpha = 90°$ (d), $2\alpha = 120°$ (e) and $2\alpha = 135°$ (f).

Table 5
Values of parameters φ and ψ obtained by fitting the data shown in Fig. 7

	$2\alpha = 30°$	$2\alpha = 45°$	$2\alpha = 60°$	$2\alpha = 90°$	$2\alpha = 120°$	$2\alpha = 135°$
φ	1.0433	1.0246	1.0144	1.0105	1.0229	1.0264
ψ	0.2409	0.226	0.2003	0.1268	0.0508	0.0246

Fig. 8. Plots of φ and ψ as a function of the notch angle 2α.

Fig. 9. Comparison along the notch bisector between predicted distributions of σ_y, based on Eqs. (5), (21) and (22), and FE results. Notch root radius equal to 0.4 mm (a) and 3.2 mm (b).

$2\alpha = 135°$. Theoretical predictions for σ_θ stress component were then obtained from Eqs. (5) and (16). The comparison is found to be very satisfactory.

6. Further considerations on the use of generalised N-SIFs

The main aim of the paper is to create a bridging between the parameters governing the stress fields of sharp V-notches and the parameters governing the stress fields of blunted V-notches. It is also possible to apply the definition given by Eq. (12) to other type of notches by using the "equivalent V-notch" concept (Filippi and Lazzarin, 2004). Some results are shown in Fig. 10 where Eq. (12) is applied to three circular and semicircular notches.

Fracture criteria for elements with V-notches are a different matter. To ascertain the limits of applicability of a fracture criterion based on critical values of $K_{\rho,\mathrm{I}}^{\mathrm{V}}$ is beyond the scope of this paper. It is reasonable to think that a fracture criterion for blunted V-notches will be valid only when the stress distribution near the blunted notch still remains close to the stress field of sharp V-notches. Just to demonstrate a possible use of Eqs. (12) and (14) we have reconsidered here a set of experimental data which were recently published by Gogotsi (2003). Those data were obtained from specimens made of ceramics. They showed a large variability of fracture toughness as a function of the V-notch root radius, which ranged from 0 to about 100 μm. The behaviour of the materials was perfectly brittle, therefore it is possible to impose $K_{\rho,\mathrm{I}}^{\mathrm{V}}$ equal to the experimental values of fracture toughness for different values of ρ, and to determine the critical value of the external load P_{CR} able to assure the required local stress distribution by means of linear elastic FE analyses. The results for silicon nitride Si_3N_4 are shown in Fig. 11 where experimental results and theoretical predictions are compared.

In the presence of sharp V-notches the influence of the notch opening 2α is fully included into N-SIF definitions. This influence is generally neglected dealing with common notches. According to Nisitani (1992), linear Notch Mechanics is an engineering method dealing with the notch problems by elastic stress fields represented by the notch root value ρ and the maximum principal stress $\sigma_{\max}$. That theory states that two notched bodies having the same ρ and the same $\sigma_{\max}$ at the notch tip are characterised by the same linear elastic stress fields. The same elastic stress field and the same response against plasticity assure the occurrence of the same elastic–plastic stress field in two notched bodies and, then, the same localised damage (Nisitani, 1992). Nisitani's statements are unquestionable for most notches of interest, but not for all notches in general. Consider two V-shaped notches different opening angles and the same value of ρ (typically, welded joints exhibit at the weld toes mean values of 2α ranging from about 110° to about 150° and a very small value of ρ). The constancy of ρ and $\sigma_{\max}$ assures the constancy of the elastic stress fields along the notch bisector only for a distance less than 0.3ρ (Atzori et al., 2001). The constancy of the linear elastic
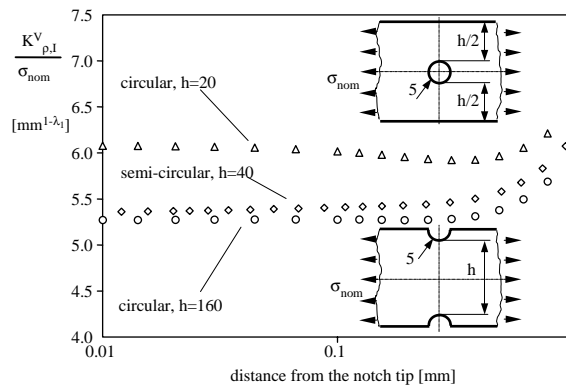

Fig. 10. Plots of $K_{\rho,\mathrm{I}}^{\mathrm{V}}$, Eq. (12), along the notch bisector of some circular and semicircular notches with $\rho = 5$ mm. The equivalent V-notches are characterized by $2\alpha = 70°$ ($1 - \lambda_1 = 0.480$), according to Filippi and Lazzarin (2004).
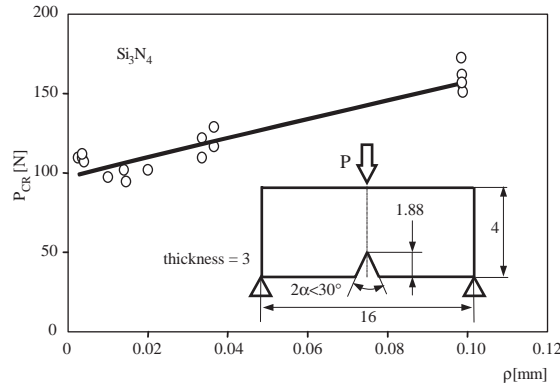
Fig. 11. Comparison between experimental and estimated values of the critical loads (Berto et al., 2005).

stress field over a more extended region needs the same opening angle, the same ρ and the same $\sigma_{\max}$. More simply, it needs the same generalised N-SIF.

7. Conclusions

In the presence of sharp V-notches (where the notch root radius is null) subjected to mode I loading conditions, the notch stress intensity factors K_I^V are recognized as parameters suitable for controlling the static behavior of brittle materials and the fatigue crack initiation phase of structural materials. When the notch root radius is different from zero, the characteristic, singular, sharp-notch field diverges from the rounded-notch solution very next to the notch. As the notch root radius ρ increases, the usefulness of K_I^V rapidly decreases.

The paper proposed a new definition of the notch intensity factor, $K_{\rho,I}^V$, based on the analytical stress distribution ahead of the V-notch tip. The new parameter quantifies the stress redistribution due to the rounded notch on the process zone, but it maintains the same units of K_I^V, $MPa(m)^{1-\lambda_1}$, where $1 - \lambda_1$ is the degree of singularity of the sharp solution. The size of the region controlled by $K_{\rho,I}^V$ was found to be mainly dependent on the notch depth, resulting in approximately one tenth of the notch depth when evaluated along the notch bisector.

Due to its nature, the new parameter might be useful in all cases where: (a) the effect of stress redistribution due to the notch root radius cannot be neglected; (b) the root radius, in combination only with the maximum principal stress at the notch tip, is not large enough to control the fracture of brittle or quasi-brittle materials, nor the fatigue crack initiation phase. Afterwards, also the intensity of the mode II stress field has been quantified by means of the parameter $K_{\rho,II}^V$, defined here on the basis of the $\tau_{r\theta}$ stress component ahead of the notch, in the impossibility to use the $\tau_{r\theta}$ stress component at the notch tip (which is null).

Since the new definitions are based on an approximate analytical frame recently reported in the literature, the accuracy of the new definitions have been carefully checked against numerical analyses. In particular, the variability of $K_{\rho,I}^V$ was found to be weak in more than 20 models analyzed numerically and this fact makes the new parameter of practical interest.

With reference only to mode I load conditions, some diagrams were reported in the paper for six different notch angles ($2\alpha = 30°$, $45°$, $60°$, $90°$, $120°$ and $135°$). These diagrams give the $K_{\rho,I}^V/K_I^V$ ratio (notch intensity factor for blunted V-notches on notch intensity factor for sharp V-notches) as a function of ρ/a, ρ and a being the notch root radius and the notch depth, respectively.

The diagrams show that:

- for each notch angle, a single curve summarizes with reasonable approximation the link between $K_{\rho,\mathrm{I}}^{\mathrm{V}}/K_{\mathrm{I}}^{\mathrm{V}}$ and ρ/a, but only when the ligament width to notch root ratio h/ρ is equal to or greater than 5.0; otherwise, the effect of the ligament width cannot be disregarded;
- by keeping ρ/a constant, the difference between $K_{\rho,\mathrm{I}}^{\mathrm{V}}/K_{\mathrm{I}}^{\mathrm{V}}$ strongly depends on the notch angle 2α; the smaller the angle, the greater the difference.

Acknowledgements

References

Atzori, B., Lazzarin, P., Tovo, R., 1999. From the local stress approach to fracture mechanics: a comprehensive evaluation of the fatigue strength of welded joints. Fatigue and Fracture of Engineering Materials and Structures 22, 369–381.

Atzori, B., Lazzarin, P., Filippi, S., 2001. Cracks and notches, analogies and differences of the relevant stress distributions and practical consequences in fatigue limit predictions. International Journal of Fatigue 23, 355–362.

Berto, F., Gogotsi, G.A., Lazzarin, P., 2005. Generalised Intensity factors applied to fracture toughness data from V-notches with small root radii. On CD-Rom, ICF 11, Int Conference on Fracture 2005, Turin.

Bogy, D.B., 1971. Two edge-bonded elastic wedges of different materials and wedge angles under surface tractions. Journal of Applied Mechanics 38, 377–386.

Carpinteri, A., 1987. Stress singularity and generalised fracture toughness at the vertex of re-entrant corners. Engineering Fracture Mechanics 26, 143–155.

Chen, D.H., 1995. Stress intensity factors for V-notched strip under tension or in-plane bending. International Journal of Fracture 70, 81–97.

Chen, D.H., 1998. Evaluation of static strength by the application of stress intensity factor for a V-shaped notch. In: Allison, I.M. (Ed.), Procs. 11th International Conference on Experimental Mechanics, Oxford, UK. A.A. Balkema Publishers, Rotterdam/Brookfield, pp. 1161–1166.

Creager, M., Paris, PC., 1967. Elastic field equations for blunt cracks with reference to stress corrosion cracking. International Journal of Fracture Mechanics 3, 247–252.

Dini, D., Hills, D., 2004. Asymptotic characterisation of nearly-sharp notch root stress fields. International Journal of Fracture 130, 651–666.

Dunn, M.L., Suwito, W., Cunningham, S.J., 1997a. Fracture initiation at sharp notches: correlation using critical stress intensities. International Journal of Solids and Structures 34, 3873–3883.

Dunn, M.L., Suwito, W., Cunningham, S.J., May, C.W., 1997b. Fracture initiation at sharp notches under mode I, mode II, and mild mixed mode loading. International Journal of Fracture 84, 367–381.

Fett, T., 1996. Failure of brittle materials near stress singularities. Engineering Fracture Mechanics 53, 511–518.

Filippi, S., Lazzarin, P., 2004. Distributions of the elastic principal stress due to notches in finite size plates and rounded bars uniaxially loaded. International Journal of Fatigue 26, 377–391.

Filippi, S., Lazzarin, P., Tovo, R., 2002. Developments of some explicit formulas useful to describe elastic stress field ahead of the notches. International Journal of Solids and Structures 39, 4543–4565.

Glinka, G., 1985. Calculation of inelastic notch-tip strain–stress histories under cyclic loading. Engineering Fracture Mechanics 22, 839–854.

Gogotsi, G.A., 2003. Fracture toughness of ceramics and ceramic composites. Ceramics International 29, 777–784.

Gómez, F.J., Elices, M., 2003a. Fracture of components with V-shaped notches. Engineering Fracture Mechanics 70, 1913–1927.

Gómez, F.J., Elices, M., 2003b. A fracture criterion for sharp V-notched samples. International Journal of Fracture 123, 163–175.

Gómez, F.J., Elices, M., 2004. A fracture criterion for blunted V-notched samples. International Journal of Fracture 127, 239–264.

Gross, R., Mendelson, A., 1972. Plane elastostatic analysis of V-notched plates. International Journal of Fracture Mechanics 8, 267–276.

Irwin, G.R., 1958. Fracture. In: Handbuch der Physik 6, Springer-Verlag, Berlin, pp. 551–590.

Knesl, Z., 1991. A criterion of V-notch stability. International Journal of Fracture 48, R79–R83.

Lazzarin, P., Livieri, P., 2001. Notch stress intensity factors and fatigue strength of aluminium and steel welded joints. International Journal of Fatigue 23, 225–232.

Lazzarin, P., Tovo, R., 1996. A unified approach to the evaluation of linear elastic fields in the neighbourhood of cracks and notches. International Journal of Fracture 78, 3–19.

Lazzarin, P., Tovo, R., 1998. A notch stress intensity factor approach to the stress analysis of welds. Fatigue and Fracture of Engineering Materials and Structures 21, 1089–1103.

Lazzarin, P., Zambardi, R., 2001. A finite-volume-energy based approach to predict the static and fatigue behaviour of components with sharp V-shaped notches. International Journal of Fracture 112, 275–298.

Murakami, Y. (Ed.), 2001. Stress Intensity Factors Handbook, vol. 5. The Society of Material Science/Elsevier, Japan, pp. 1773–1877.

Neuber, H., 1958. Theory of Notch Stresses. Springer-Verlag, Berlin.

Nisitani, H., 1992. Measure of severity controlling the localized damage in a crack or a notch. In: Computational Methods in Fracture Mechanics, Computational Mechanics Pub., vol. 2, pp. 567–580.

Nui, L.S., Chehimi, C., Pluvinage, G., 1994. Stress field near a large blunted tip V-notch and application of the concept of the critical notch stress intensity factor (NSIF) to the fracture toughness of very brittle materials. Engineering Fracture Mechanics 49, 325–335.

Reedy Jr., E.D., 1993. Asymptotic interface-corner solutions for butt tensile joints. International Journal of Solids and Structures 30, 767–777.

Reedy Jr., E.D., Guess, T.R., 1993. Comparison of butt tensile strength data with interface corner stress intensity factor prediction. International Journal of Solids and Structures 30, 2929–2936.

Seweryn, A., 1994. Brittle fracture criterion for structures with sharp notches. Engineering Fracture Mechanics 47, 673–681.

Seweryn, A., Mróz, Z., 1995. A non-local stress failure condition for structural elements under multiaxial loading. Engineering Fracture Mechanics 51, 955–973.

Seweryn, A., Poskrobko, S., Mróz, Z., 1997. Brittle fracture in plane elements with sharp notches under mixed-mode loading. Journal of Engineering Mechanics 123, 535–543.

Susmel, L., Taylor, D., 2003. Two methods for prediction the multiaxial fatigue limits of sharp notches. Fatigue and Fracture of Engineering Materials and Structures 26, 821–833.

Strandberg, M., 2002. Fracture at V-notches with contained plasticity. Engineering Fracture Mechanics 69, 403–415.

Williams, M.L., 1952. Stress singularities resulting from various boundary conditions in angular corners of plates in extension. Journal of Applied Mechanics 19, 526–528.